FEBS Open Bio 4 (2014) 510–521

FEBS openbio

journal homepage: www.elsevier.com/locate/febsopenbio

Structural and degradative aspects of ornithine decarboxylase antizyme inhibitor 2

Bruno Ramos-Molina [a,e], Ana Lambertos [a,e], Andrés J. Lopez-Contreras [b], Joanna M. Kasprzak [c], Anna Czerwoniec [c], Janusz M. Bujnicki [d], Asunción Cremades [a,e], Rafael Peñafiel [a,e,*]

[a] Department of Biochemistry and Molecular Biology B and Immunology, University of Murcia, Spain
[b] Genomic Instability Group, Spanish National Cancer Research Centre (CNIO), Madrid, Spain
[c] Institute of Molecular Biology and Biotechnology, Adam Mickiewicz University, Poznan, Poland
[d] International Institute of Molecular and Cell Biology, Warsaw, Poland
[e] Instituto Murciano de Investigación Biosanitaria (IMIB), Murcia, Spain

ARTICLE INFO

Article history:
Received 13 May 2014
Revised 23 May 2014
Accepted 27 May 2014

Keywords:
Antizyme
Antizyme-binding element
Homology modeling
Polyamines
Protein degradation
Proteasome inhibitors

ABSTRACT

Ornithine decarboxylase (ODC) is the key enzyme in the polyamine biosynthetic pathway. ODC levels are controlled by polyamines through the induction of antizymes (AZs), small proteins that inhibit ODC and target it to proteasomal degradation without ubiquitination. Antizyme inhibitors (AZIN1 and AZIN2) are proteins homologous to ODC that bind to AZs and counteract their negative effect on ODC. Whereas ODC and AZIN1 are well-characterized proteins, little is known on the structure and stability of AZIN2, the lastly discovered member of this regulatory circuit. In this work we first analyzed structural aspects of AZIN2 by combining biochemical and computational approaches. We demonstrated that AZIN2, in contrast to ODC, does not form homodimers, although the predicted tertiary structure of the AZIN2 monomer was similar to that of ODC. Furthermore, we identified conserved residues in the antizyme-binding element, whose substitution drastically affected the capacity of AZIN2 to bind AZ1. On the other hand, we also found that AZIN2 is much more labile than ODC, but it is highly stabilized by its binding to AZs. Interestingly, the administration of the proteasome inhibitor MG132 caused differential effects on the three AZ-binding proteins, having no effect on ODC, preventing the degradation of AZIN1, but unexpectedly increasing the degradation of AZIN2. Inhibitors of the lysosomal function partially prevented the effect of MG132 on AZIN2. These results suggest that the degradation of AZIN2 could be also mediated by an alternative route to that of proteasome. These findings provide new relevant information on this unique regulatory mechanism of polyamine metabolism.

1. Introduction

Polyamines are small cationic molecules essential for cell growth, proliferation, differentiation and apoptosis [1–4]. In mammals, the intracellular polyamine levels are tightly controlled by the regulation of different processes including their biosynthesis, degradation and transport across the plasma membrane [5]. Ornithine decarboxylase (ODC) is the key biosynthetic enzyme that converts ornithine into putrescine, which is the precursor for the physiological polyamines, spermidine and spermine. Different studies have revealed that ODC and polyamines play an important role in the development of cancer [6–8]. ODC activity is highly dependent on the intracellular polyamine concentrations, being rapidly down regulated under high polyamine amounts, acting at transcriptional, translational and post-translational levels [9]. Post-translational regulation of ODC is mainly mediated by the action of a family of small proteins named antizymes (AZs), whose synthesis is stimulated by increased polyamine levels [10]. AZs bind and inhibit ODC and target it to proteasomal degradation without ubiquitination [11,12]. Besides, AZs inhibit extracellular polyamine uptake presumably by interacting with the polyamine transport system [13–15]. In mammals, the family of AZs is composed by three isoforms (AZ1-3), AZ1 being the most predominant

Abbreviations: AZ, antizyme; AZBE, antizyme-binding element; AZIN, antizyme inhibitor; ERGIC, endoplasmic reticulum-Golgi intermediate compartment; ODC, ornithine decarboxylase; GDT_TS, global distance test total score; HA, hemagglutinin; HEK, human embryonic kidney; PAGE, polyacrylamide gel electrophoresis; RMSD, root-mean-square deviation; TGN, trans-Golgi network

* Corresponding author. Address: Department of Biochemistry and Molecular Biology B and Immunology, Faculty of Medicine, University of Murcia, 30100 Murcia, Spain. Tel.: +34 868 88 7174.
E-mail address: rapegar@um.es (R. Peñafiel).

http://dx.doi.org/10.1016/j.fob.2014.05.004
2211-5463/

form in most cells and tissues [16,17]. Despite the fact that all AZ isoforms are able to inhibit ODC and the polyamine uptake, only AZ1 clearly induces ODC proteasomal degradation [11,18]. In fact, there are controversial data on the capacity of AZ2 for targeting ODC to degradation *in vivo* and *in vitro* [19–21], and recently it has been reported that AZ3, a testis-specific isoform [22,23], is unable to target ODC to degradation [21].

In addition to AZs, the ODC activity is also indirectly regulated by a family of proteins named antizyme inhibitors (AZINs). These proteins, closely related to ODC but without enzymatic activity, also interact with antizymes, even more efficiently than ODC, counteracting the effects of antizymes on ODC [24,25]. In mammals, the AZIN family is formed by two members: AZIN1 and AZIN2. AZIN1 is a ubiquitous protein that regulates intracellular polyamine levels and cell growth [26–29]. Mice with disruption of the AZIN1 gene die soon after birth [30]. On the other hand, AZIN2 was first found to be expressed in testis and brain [31,32], but more recent analyses have indicated that it is also expressed in specific type of cells and secretory tissues [33–36]. Although the physiological role of AZIN2 is mostly unknown, there are data suggesting that it is involved in cell growth, vesicular trafficking, secretion and spermiogenesis [36–39]. Interestingly, overexpression of AZIN2 has been observed in certain pathologies [40].

Numerous studies have demonstrated that ODC is enzymatically active as homodimer [9,41,42], and that in solution there is an equilibrium between the monomeric inactive form and the dimeric one [41,43]. It is also well known that antizyme exerts its negative effect on ODC activity by binding to the ODC monomer, preventing the formation of the active ODC dimer, and by targeting the inactive ODC to the 26S proteasome, where ODC is degraded without ubiquitination [11]. Initial studies based on the differential affinity for AZ between murine and trypanosomal ODC, led to the identification of the antizyme-binding element (AZBE), as a sequence spanning the residues from 117 to 140 in mouse ODC [44]. Subsequently, the analysis of the tertiary structure of ODC revealed that this region is present in two α-helices included in a TIM-like α/β-barrel domain, in which several basic residues are exposed toward the surface [45,46]. On the other hand, although AZIN1 has been crystallized as a dimer, it has been detected in a monomeric state under physiological conditions [47]. Like ODC, AZIN1 binds to AZs through the AZBE region but in this case the binding to AZs makes AZIN1 more resistant against proteasomal degradation, probably because AZs inhibit its ubiquitination [48]. The interaction between ODC or AZIN1 with AZ1 through the AZBE region has been computationally predicted by docking, the models being quite similar in both cases [49]. Although the amino acid sequences of the AZBE region of ODC and AZIN1 are quite similar, differences in residues 125 and 140 have been related with their differential AZ-binding affinity [50].

In comparison to ODC and AZIN1, little is known about the molecular aspects of the interaction between AZIN2 and AZs, probably due to the lack of information on AZIN2 structure. In addition, the limited information related to AZIN2 degradation and interaction with AZs has been mostly obtained from *in vitro* assays. Due to the potential relevance of AZIN2 in the physiology of differentiated cells, the aim of this work was to analyze structural and functional properties of AZIN2, and determine their impact on the interaction with AZs and the stability of the protein.

2. Results

2.1. Biochemical studies demonstrate that AZIN2 exists as a monomer

For this purpose, we used HEK 293T cells transfected with AZIN2-FLAG, and compared the results with those obtained for ODC-FLAG under the same experimental conditions. Cross-linking analysis clearly showed, as expected, the presence of ODC dimers (Fig. 1A). In the case of AZIN2, the putative dimer band was not detected. However, after the cross-linking reaction the monomer band almost disappeared, detecting faint staining of bands corresponding to higher molecular weight than the putative dimer (Fig. 1A). Since AZIN2 is located in the endoplasmic reticulum-Golgi intermediate compartment (ERGIC) and in the trans-Golgi network (TGN) [39,51], these higher molecular weight bands may correspond to cross-linked species of the AZIN2 monomer with membrane proteins of these compartments, to which AZIN2 is likely to be associated. Interestingly, when AZIN2 was co-transfected with AZ1, after cross-linking experiments the main band of AZIN2 detected was mainly the monomer, probably due to the fact that AZ1 prevents the binding of AZIN2 to proteins of the outer surface of the ERGIC or the Golgi apparatus, in agreement with previous data [39,51], and therefore, the formation of the cross-linked species of higher molecular weight. To corroborate the monomeric state of AZIN2 under physiological conditions, we next studied cell extracts of transfected cells with AZIN2 (or ODC), using polyacrylamide gel electrophoresis (PAGE) under non-denaturing conditions. Fig. 1B shows that whereas in the case of ODC two bands were found, corresponding to monomeric and dimeric forms of ODC, only the lower molecular weight band corresponding to the monomer was detected for AZIN2. Finally, size exclusion chromatography was used to analyze the size of transfected AZIN2 and

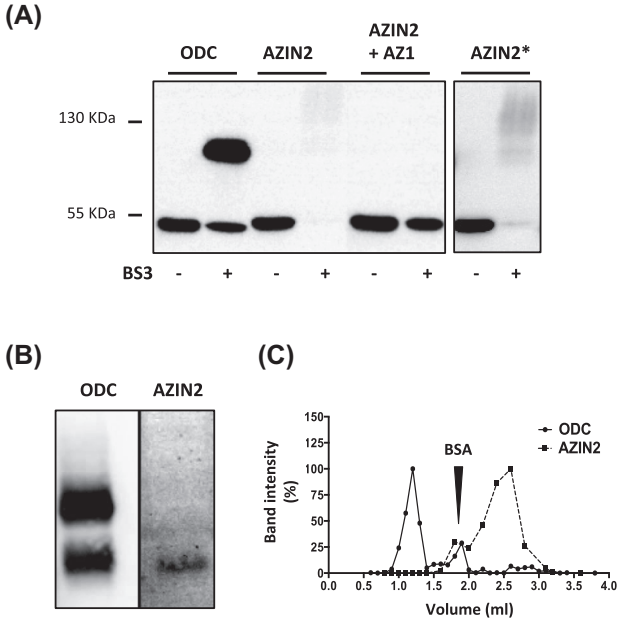

Fig. 1. Biochemical studies of the AZIN2 quaternary structure in transfected cells. (A) Left panel: Cross-linking analysis of transfected cell lysates of AZIN2 and ODC. HEK 293T cells were transiently transfected with AZIN2-FLAG, ODC-FLAG, or co-transfected with AZIN2-FLAG and AZ1, and the cell lysates were incubated with 1 mM bissulfosuccinimidylsuberate (BS3) for 1 h. The proteins were then separated by SDS-PAGE, transferred onto PVDF membrane, which was then incubated with an anti-FLAG antibody. Note that the band corresponding to AZIN2 monomers disappears after cross-linking. Right panel (marked with an asterisk): AZIN2 blot similar to that shown in the left panel, but using a longer exposure time to the detection reagent. Note that the tag is now found in high molecular weight bands. (B) Migration pattern of AZIN2-FLAG and ODC-FLAG under native conditions. Samples were analyzed by non-denaturing PAGE, blotted to PVDF and probed with an anti-FLAG antibody. (C) Size-exclusion chromatography of AZIN2-FLAG and ODC-FLAG. AZIN2-FLAG or ODC-FLAG cell lysates were resolved by a gel filtration column (Zorbax GF-250) and fraction aliquots were analyzed by Western blot or assayed for ODC activity. The arrowhead marks the elution fraction in which bovine serum albumin (BSA) was eluted.

ODC products. Fig. 1C shows that the elution profiles of ODC and AZIN2 were different. Thus, whereas ODC migrated mainly as a dimer, AZIN2 was only found as a monomer.

Although all these results pointed out for the inability of AZIN2 to form homodimers, in contrast to ODC, we wondered whether AZIN2 may form heterodimers with ODC. To answer this question we carried out immunoprecipitation assays using cells co-transfected with constructs of AZIN2 tagged with the FLAG epitope (AZIN2-FLAG) and ODC tagged either with the hemagglutinin epitope (ODC-HA) or the FLAG epitope (ODC-FLAG). Fig. 2A shows that in cells co-transfected with both ODC constructs, dimers formed by ODC-HA and ODC-FLAG monomers could be detected by Western blotting after co-immunoprecipitation. However, no evidence of heterodimer formation between AZIN2 and ODC was found in the cells co-transfected with AZIN2-FLAG and ODC-HA. In agreement with these results, ODC activity was not decreased by co-transfection with AZIN2 (Fig. 2B). Note that the formation of AZIN2-ODC heterodimers would have decreased the activity of ODC due to the lack of decarboxylating activity of AZIN2 [32,52].

2.2. Prediction of the 3D structure of murine AZIN2 monomer by homology modeling

The 3D structure of ODC, the rate-limiting enzyme of polyamine biosynthesis, has been previously characterized in mouse, human and *Trypanosoma brucei* [45,46,53]. In all cases the structure is composed of two well-defined domains: a TIM-like α/β-barrel, formed by eight α-helices and eight β-strands, and a β-sheet domain. Because ODC crystallized as a dimer, the residues involved in the interface between monomers have been well characterized [45]. In addition, the 3D structure of mouse AZIN1 has also been recently determined [47]. Although AZIN1 crystallized as a dimer, subsequent experiments demonstrated that AZIN1 exists as a monomer in solution under physiological conditions [47]. Little is known on the structure of AZIN2, the recently characterized ODC paralogue [32], since no AZIN2 crystals have been obtained so far. However, due to the high sequence similarity of AZIN2 to ODC and AZIN1 (48% and 37% sequence identity, respectively), AZIN2 is an excellent candidate to be modeled using the comparative modeling approach.

Full-length sequence of murine AZIN2 was submitted to the Genesilico Metaserver [54]. Protein fold-recognition methods detected, as the closest relatives with known structures, the mouse ODC (PDB: 7odc) and mouse AZIN1 (PDB: 3btn). Both template structures exhibited segments missing in crystals, for which coordinates were not available: loops 30–35, 158–168 and 298–311 and last 37 residues in the C-terminus in ODC and the N-terminus (residues 1–7), loops 160–167, 294–310 and 330–334 and the last 13 residues in the C-terminus in AZIN1. To increase the structural coverage, we carried out comparative modeling using both templates. The preliminary model of AZIN2 was generated by using the automated protein modeling program Modeller [54], and its local accuracy was predicted by MetaMQAPII [55]. Two loops comprising residues 160-167 and 298–310, and 13 N-terminal residues were predicted to be poorly folded, hence the model was subjected to local optimization, using *de novo* loop modeling approach implemented in Refiner [56]. The resulting final model (Fig. 3A and B) obtained the LG score of 5.219 according to ProQ [57], which indicates a potentially "extremely good model", which is also in agreement with scores predicted by GDT_TS (70.207) and RMSD (3.002) according to MetaMQAPII assessment. Furthermore, another important domain for the subcellular localization of AZIN2, the region formed by residues 70–110 [51], is also included between two helices and a β-strand in the same α/β-barrel. The close proximity of these two domains may explain that after binding to AZs, the interaction of AZIN2 with the outer surface of the ERGIC membranes may be hindered. Fig. 3C shows the predicted 3D structure of AZIN2 in which the residues 70–110 and 111–145 are highlighted in red and yellow, respectively. Like ODC and AZIN1, in AZIN2 the AZBE region (111–145) is mainly formed by two α-helices and one β-strand, all of them included in a TIM-like α/β-barrel.

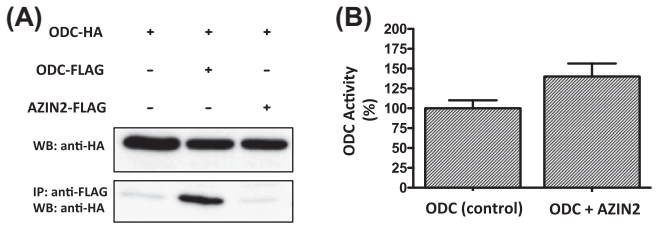

Fig. 2. (A) AZIN2 is unable to form heterodimers with ODC. Cells were transfected with ODC-HA or co-transfected with ODC-HA and AZIN2-FLAG or ODC-FLAG. Samples from cell lysates were analyzed by Western blot using an anti-HA antibody. In addition, samples were inmunoprecipitated (IP) with anti-FLAG affinity gel beads for 3 h. After washing, the eluted proteins were subjected to Western blot analysis and incubation with an anti-HA antibody (lower row). ODC-FLAG but not AZIN2-FLAG interacted with ODC-HA. The blots shown are representative of three experiments. (B) ODC activity in cells transfected with ODC alone or in presence of AZIN2.

2.3. Mutational analysis reveals the influence of conserved residues in the AZBE region of AZIN2 on the interaction with AZ1

Although we initially reported that AZIN2 interacts with the three antizymes [32], little is known on the molecular aspects of this interaction. In ODC, an important structural element for the binding to antizymes is the AZBE domain. This region was early identified by comparing trypanosomal ODC, an enzyme isoform that is not regulated by AZ, with mouse ODC [44]. The AZBE site spans from residues 117 to 140 of mouse ODC. In a previous work, we found that the deletion of this sequence abolished the capacity of AZIN2 to stimulate polyamine uptake, presumably because this variant does not interact with AZs [58]. In order to determine the residues of the AZBE region of AZIN2 implicated in the interaction with AZs, we considered the five conserved amino acid residues (K116, A124, E139, L140 and K142) of this region in mouse AZIN2 (Fig. 4A), previously deduced [59] by using a multi-alignment sequence analysis of the AZBE region of AZIN2 orthologues and those of corresponding paralogues provided by the ENSEMBL genome database. Given that several conserved acidic glutamate residues are present in the region of AZ1 necessary for the interaction with ODC [60] and that the putative AZBE site of ODC contains various basic residues, one might expect an electrostatic binding between AZ1 and ODC. In agreement with this hypothesis, a recent study has associated the electric charge of the AZBE site to the interaction ODC-AZ1 [61]. In the case of mouse AZIN2 the total charge of the putative AZBE site is +2, due to the presence of five basic (K116, K122, K126, R130 and K142) and three acidic residues (D135, E137 and E139) (see Fig. 4A). Note that two of the conserved residues are positively charged lysines (K116 and K142) that could interact electrostatically with the conserved glutamic residues of AZ1. To determine the influence of the electric charge on the interaction between AZIN2 and AZ, we first specifically generated several AZIN2 variants by substituting conserved lysine or glutamic residues by neutral uncharged alanines. Thus, we obtained several single, double and triple substitutions in which the electric charge was maintained (A124S; L140A; E139A/L140A/K142A), reduced (K116A; K142A; K116A/K142A) or increased (E139A; E139A/L140A) (see Fig. 4B).

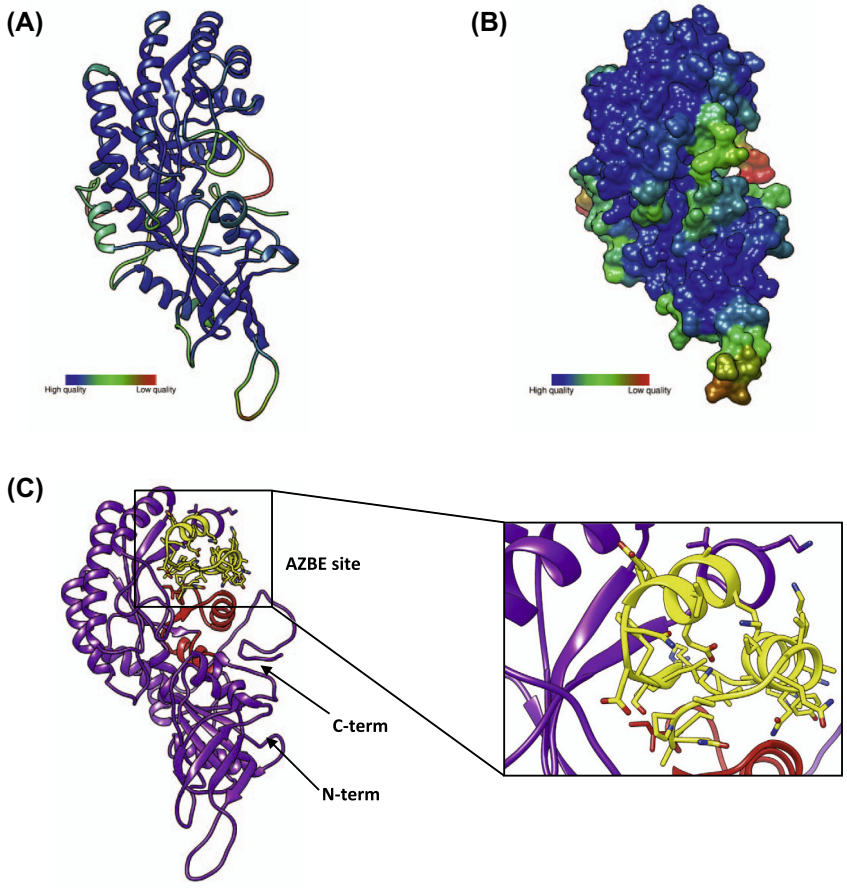

Fig. 3. Structural model of mouse AZIN2. The upper row presents the predicted model in the ribbon (A) and the surface (B) representation, colored according to the predicted local deviation from the real structure (i.e., the predicted error of the model), as calculated by MetaMQAPII: blue indicates low predicted deviation of Cα atoms down to 0 Å, red indicates unreliable regions with deviation >5 Å, green indicates intermediate values. (C) Predicted tertiary structure of AZIN2 in the ribbon representation with the AZBE region in yellow and the N terminus region formed by the 70–110 residues in red. The side chains of the amino acids included in the AZBE region (111–145) were also shown and colored according to the type of atom (red, oxygen; blue, nitrogen).

To quantify the direct interaction of AZ1 with AZIN2 we carried out immunoprecipitation experiments using co-transfected cell lysates. Fig. 5A shows that whereas the variants with single alanine substitutions K116A (K1A) and K142A (K2A) clearly interacted with AZ1, almost similarly as wild type AZIN2, a weak signal was detected in the case of the variant bearing a double substitution K116A/K142A (KK/AA), suggesting that the elimination of the positive charge in the AZBE region negatively affects the interaction of AZIN2 with AZ1. Additionally, as expected, no signal was observed for the AZBE-deleted variant, since this protein lacks the structural domain responsible for AZ binding. In order to test if the electric charge of the AZBE region is the only factor responsible for the interaction or whether the electro neutral substitution of the conserved residues may affect such interaction, we tested the binding of AZ1 to a variant with a triple substitution E139A/L140A/K142A (ELK/AAA). In this variant the conserved residues E139, L140 and K142 had been substituted by alanines, but it still retains a net charge of +2 in the AZBE region. As shown in Fig. 5A the binding of this variant to AZ1 was markedly lower than in the case of the wild type or the single-substitution variant. This result suggests that not only the charge but also the presence of critical conserved residues are important for the interaction of AZIN2 with AZ1.

To confirm this hypothesis, we generated additional protein variants by substituting individually the residues E139 and L140 for alanines, and A124 for serine. We also obtained a variant with a double substitution E139A/L140A (EL/AA) in order to determine the importance of both residues respect to the variant with the triple substitution ELK/AAA in which K142 was also substituted. The effect of these substitutions on the AZIN2-AZ interaction was tested by immunoprecipitation experiments (Fig. 5B). The variant A124S markedly interacted with AZ1, similarly to the wild type protein, ruling out an important role for this residue in the binding to AZ1. The single substitutions of E139 and L140 residues to alanines only moderately reduced the interaction with AZ1. However, the variant EL/AA with a double substitution showed weaker interaction with AZ1 than the single-substitution variants but higher than the triple-substitution variant ELK/AAA. It should be noted that the variants E139A and EL/AA, although bearing an electric charge of +3, did not show increased affinity to AZ1. This suggests again that the substitution of two or more conserved residues in AZIN2 appears to be a more important factor than the reduction of the positive charge to interact with AZ1.

2.4. Substitutions of conserved residues in the AZBE region affect the biochemical functions of AZIN2

It is well known that AZIN2 increases ODC activity and polyamine uptake through the inhibition of endogenous AZ [32,37,52,58]. In order to confirm that the decreased AZ1-binding capacity shown by the described substitutions also affected AZIN2 functions, we transiently transfected HEK 293T and COS7 cells with the different constructs and the effects of these mutant forms of AZIN2 on ODC activity and polyamine uptake were studied. Fig. 6A shows that whereas wild type AZIN2 markedly increased

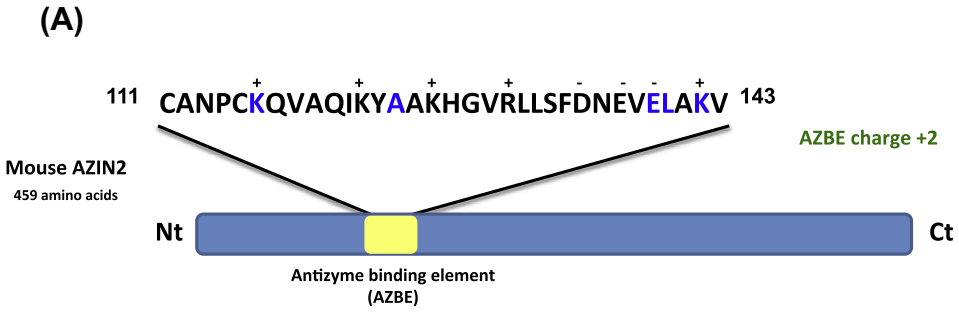

(B)

AZIN2 mutant	Abreviature	AZBE charge
K116A/K142A	KK/AA	0
K116A	K1A	+1
K142A	K2A	+1
A124S	A124S	+2
L140A	L140A	+2
E139A/L140A/K142A	ELK/AAA	+2
E139A	E139A	+3
E139A/L140A	EL/AA	+3

Fig. 4. Conserved residues of the putative AZBE region of mouse AZIN2. (A) Region encompassed by residues 117–143 of mouse AZIN2, showing the invariant residues (shown in blue) found by multiple alignment of the AZBE amino acid sequences from different AZIN2 orthologues and paralogues (ODC and AZIN1). See Ref. [59]. (B) Scheme of the different mutations in AZIN2 affecting the conserved residues of the AZBE region, and the electric charge of this region in the different AZIN2 mutants.

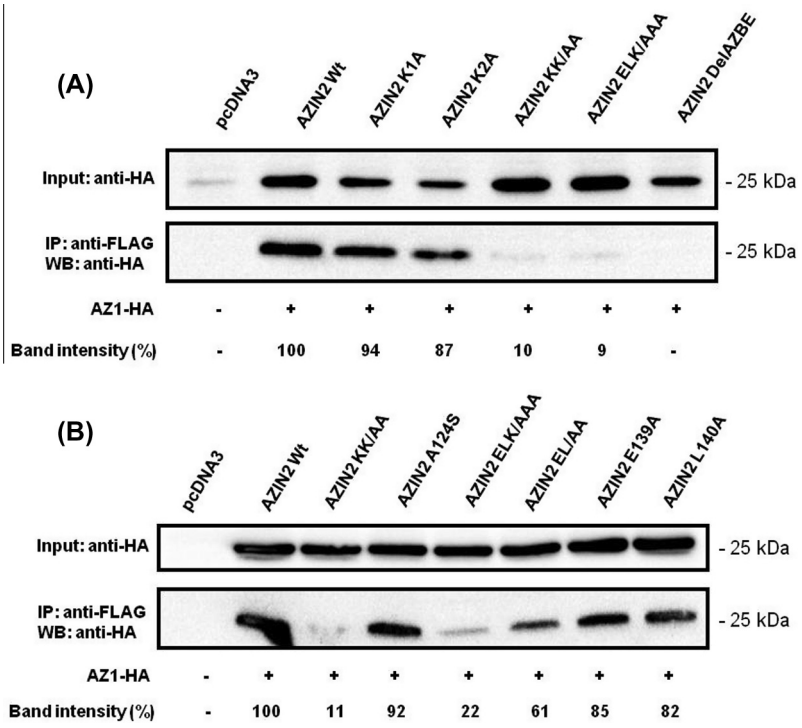

Fig. 5. Mutations of certain conserved residues of the AZBE region negatively affect the interaction of AZIN2 with AZ1. (A) HEK 293T cells were transfected with wild type AZIN2-FLAG (AZIN2 Wt), or with variants with single substitutions (K116A and K142A), double substitutions (KK/AA), triple substitutions (ELK/AAA) or with the AZBE-deleted protein (DelAZBE), together with AZ1-HA. (B) Cells were transfected with AZIN2 Wt or variants with single substitutions (A124S, E139A and L140A), double substitutions (KK/AA and EL/AA), and triple substitutions (ELK/AAA), together with AZ1-HA. The cell lysates were immunoprecipitated with anti-FLAG affinity gel beads for 3 h. After washing, the eluted proteins (IP) were separated by electrophoresis and Western blot analysis was performed. AZ1-HA was detected using an anti-HA antibody.

the decarboxylating activity of endogenous ODC in HEK 293T cells, the double-substitution variant KK/AA and the triple-substitution variant ELK/AAA, with reduced AZ-binding capacity, were not able to increase the endogenous ODC activity. In another set of experiments, using single, double and triple co-transfections with ODC, AZ1 and different constructs of AZIN2, similar results were

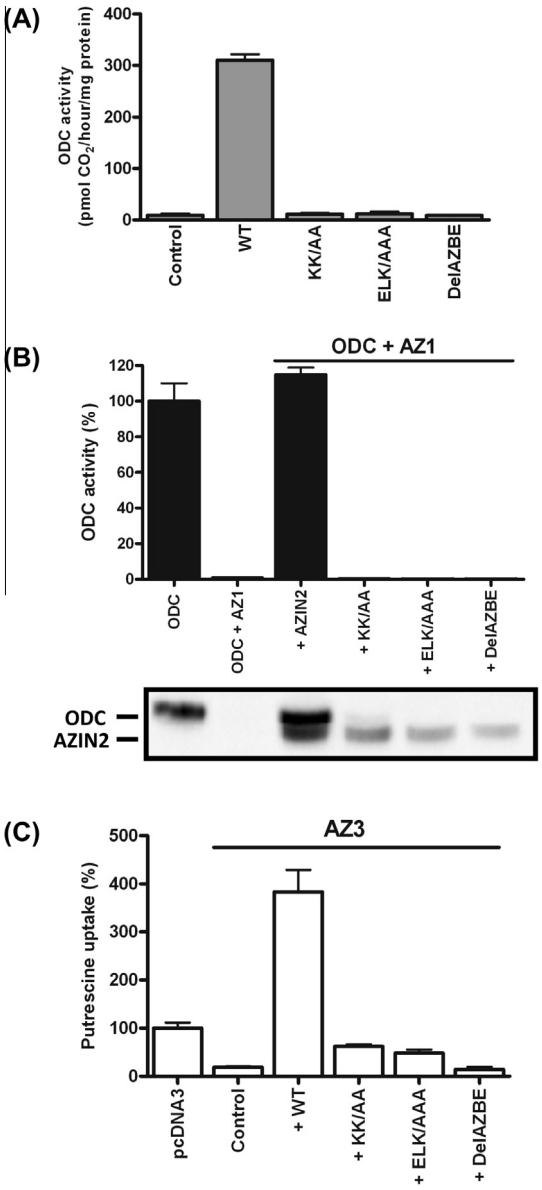

Fig. 6. AZIN2 variants were less effective than unaltered AZIN2 in regulating the polyamine homeostasis. (A) Influence of AZIN2 and its variants on the endogenous ODC activity of HEK 293T cells. The cells were transiently transfected with AZIN2 (WT) or with some AZIN2 variants. Twenty-four hours after transfection ODC activity was assayed in the cell extracts as indicated in Section 4. Control cells were transfected with the empty vector. (B) Influence of AZIN2 and its variants on ODC activity in cells co-transfected with ODC and AZ1. ODC and AZIN2 protein levels were analyzed by Western blot. The molar ratio of the different constructs (ODC-FLAG/AZIN2-FLAG/AZ) was 10:10:1. (C) Putrescine uptake by COS7 cells transfected with AZ3 or co-transfected with AZ3 and AZIN2 variants. Control cells were transfected with the empty vector. Data are expressed as mean ± S.E. of triplicate determinations.

obtained (Fig. 6B). Whereas wild type AZIN2 completely abolished the effect of AZ1 on ODC activity and protein, neither the KK/AA variant nor the ELK/AAA variant were able to abrogate the effect of AZ1 on ODC. Finally, the effect of AZIN2 and these variants on putrescine uptake was assayed in COS7 cells transfected with AZ3, because this antizyme isoform is probably an important physiological partner of AZIN2, due to that both proteins are mostly expressed in the testis [38]. Fig. 6C shows that in cells transfected with AZ3, putrescine uptake was markedly reduced and that only wild type AZIN2, but not the mutated forms of AZIN2, counteracted the negative effect of AZ3 on polyamine transport. These results indicate that the changes elicited by these substitutions in AZIN2, similarly affect the interaction of AZIN2 with both antizymes, and concomitantly the AZIN2-mediated modulation of both ODC activity and polyamine uptake.

2.5. Half-life and degradation of AZIN2. Influence of the interaction with AZs

To determine the half-life of AZIN2 and to compare this with those of ODC and AZIN1, we transiently transfected HEK 293T cells with constructs encoding the FLAG-tagged tested proteins, and after transfection the cells were incubated with cycloheximide at different times. Fig. 7A shows that under overexpression conditions the half-life of AZIN2 (~90 min) was much lower than that of ODC (>8 h), but significantly higher than that of AZIN1 (~40 min). Note that transfected ODC was quite stable in contrast to the short half-life (lower than 30 min) found for the endogenous ODC of HEK 293T cells (data not shown), probably due to the marked differences in the ODC/AZ ratio between transfected and non-transfected cells. In addition, we analyzed the effect of AZs on AZIN2 stability by means of the co-transfection of HEK 293T cells with AZIN2-FLAG and each of the three different AZs. Fig. 7B shows that the degradation of AZIN2 was reduced by the presence of any of the three AZ isoforms, but the protective effect was higher in the case of AZ1 and AZ2 ($t_{1/2}$=543 ± 93, 492 ± 99 and 155 ± 10 min in presence of AZ1, AZ2 and AZ3, respectively). Accordingly, the AZIN2 steady state levels were always higher in presence of the AZs (Fig. 7C), which is in agreement with previous works [37,38]. Although it is known that AZs are able to bind and regulate ODC [18,24], and as shown here AZs stabilize AZIN2, little is known on the effect of AZ-binding proteins on AZs stability. Fig. 8A shows that the co-expression of AZIN2 with each of the three AZs, markedly increased the steady state levels of AZs in the transfected cells, and that such stabilization of AZs was not observed when the cells were transfected with AZBE-deleted AZIN2, a mutated form of AZIN2, that, as shown in Fig 5A, is unable to bind to AZs. These results suggest that AZs and AZIN2 mutually stabilize each other by the formation of an AZ-AZIN2 complex. Similarly to AZIN2, ODC stabilized AZ2 and AZ3 but, however, the effect on AZ1 was different since ODC elicited the decrease of AZ1 protein. This discrepancy appears to be related with the degradation of ODC by the proteasome, since the co-transfection of AZ1 with the truncated form of ODC, lacking the 21 residues of the C-terminal region (ΔCt-ODC), a stable form of ODC [9], protected AZ1 from degradation as efficiently as AZIN2 (Fig. 8C).

It is known that AZINs are degraded in a ubiquitin-dependent manner by the proteasome [37,48,52], in contrast to ODC that is degraded by the proteasome without ubiquitination [11]. To obtain further information about possible differences in the degradative processes of these proteins, we incubated HEK 293T cells, transfected with the different paralogue constructs, with cycloheximide in absence and presence of the proteasome inhibitor MG132. Fig. 9A shows that the protein levels of AZIN1 and AZIN2 decreased after treatment with cycloheximide, as expected, due to the high turnover of these two proteins. However, the co-administration of cycloheximide with the proteasomal inhibitor MG132 caused differential effects on AZIN protein levels. Thus, whereas AZIN1 was not decreased under this condition, due to the inhibitory effect of MG132 on degradation, AZIN2 was still degraded. This unexpected effect of MG132 on AZIN2 was corroborated by incubating AZIN2-transfected cells with MG132 alone (Fig. 9B). To determine whether the down-regulation of AZIN2 by the proteasome inhibitor could be mediated by channeling AZIN2 to an alternative degradative route to that of the proteasome 26S, we performed a set of experiments in which the AZIN2-transfected cells were incubated simultaneously with MG132 and different inhibitors of lysosomal

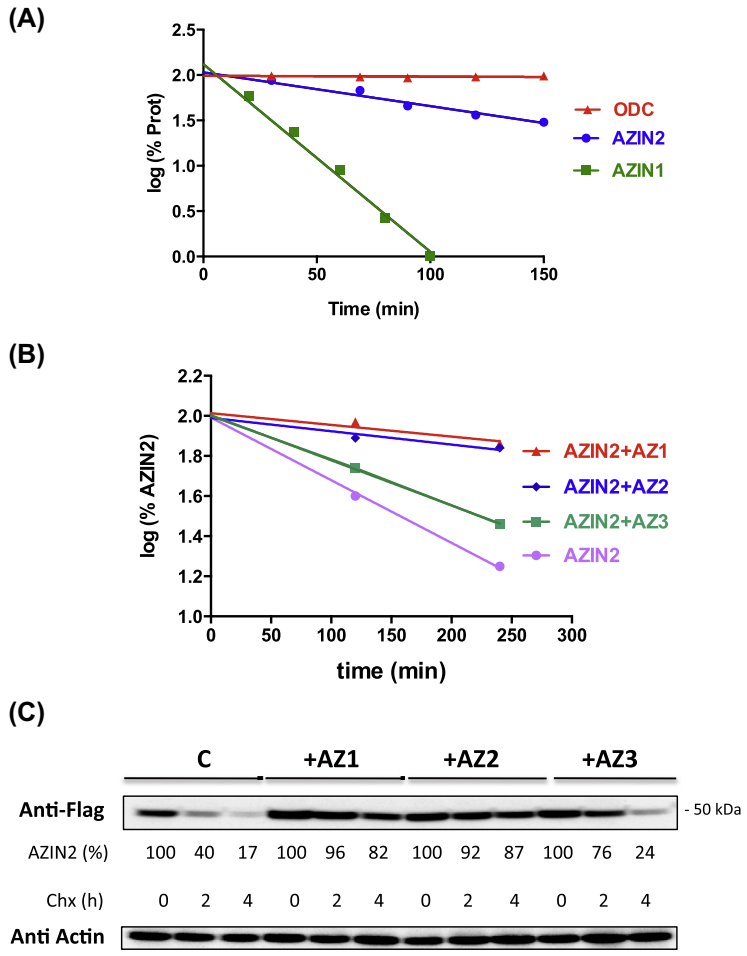

Fig. 7. Half-lives of AZIN2 and its paralogues ODC and AZIN1 in HEK 293T cells. (A) Cells were transfected with AZIN2, AZIN1 or ODC tagged with FLAG. Twenty-four hours after transfection, cycloheximide (100 μM) was added, the cells harvested at the indicated times and ODC levels were detected by measuring the enzymatic activity, whereas AZIN1 and AZIN2 protein levels were determined by Western blot analysis using an anti-FLAG antibody. (B) Influence of the AZs in the half-life of AZIN2. Cells were transfected with AZIN2-FLAG alone or co-transfected with AZIN2-FLAG and each of the three AZ isoforms. Transfected cells were treated as indicated above and protein levels were determined by Western blot analysis and incubation with anti-FLAG antibody as shown in (C). The indicated values of % degradation represent a mean value of three repetitions.

function, such as ammonium chloride and chloroquine. As shown in Fig. 9C, the inhibition of the lysosomal degradation pathway by ammonium chloride or chloroquine partially prevented the degradation of AZIN2.

3. Discussion

Although antizyme inhibitors (AZIN1 and AZIN2) and ODC share both high sequence similarity and the capacity to bind to antizymes, there are many differences between these three homologous proteins. Thus, whereas ODC has ornithine decarboxylating activity, antizyme inhibitors do not display any catalytic activity [26,32]. In addition, ODC is one of the few mammalian proteins that are degraded by the proteasome without ubiquitination [62], while antizyme inhibitors require ubiquitination [37,48]. The knowledge of the tertiary and quaternary structures of proteins is fundamental to understand their mechanism of action. Thus, in mammalian cells, monomeric and dimeric forms of ODC are in equilibrium, but only the homodimer is catalytically active [41]. In addition, only the ODC monomer is able to bind to antizymes, this step being required for its degradation by the proteasome [12]. Although the crystal structures of ODC and AZIN1 have been elucidated [45–47], and both ODC and AZIN1 crystallize as dimers, AZIN1 exists only as a monomer in solution [47].

Our results indicate that AZIN2 is mainly present as a monomer, at least in transfected cells. The cross-linking experiments also support that the AZIN2 monomer may be in close contact with other cellular proteins. These findings are in agreement with previous experiments that showed that AZIN2 is associated to membranes of the Golgi network [39,51]. In addition, the fact that co-transfection with AZ1 prevented the cross-linking of AZIN2 with such membrane proteins, may also be explained by considering that the binding to AZ1 precludes the interaction of AZIN2 with these target proteins, as suggests a preliminary docked model of the AZIN2-AZ1 complex, in which the binding of AZ1 to the AZBE domain may compete with the binding of AZIN2 to the membranes, because the partial overlapping of these two AZIN2 domains (Ramos-Molina et al., unpublished data). This is also in agreement with reported experiments in which the co-transfection of AZIN2 with antizymes shifted AZIN2 from the membranous structures to the cytosol [51]. Although our immunoprecipitation studies also indicate that AZIN2 binds to AZ1, and that this binding protects AZIN2 against degradation, we were not able to identify the putative heterodimer AZIN2-AZ1 by the cross-linking experiments. This could be due to the fact that in such complex the residues that can react with the cross-linking agent are not located at the adequate distance to allow the formation of bridges between both proteins. Interestingly, the incapacity of AZIN2 to form

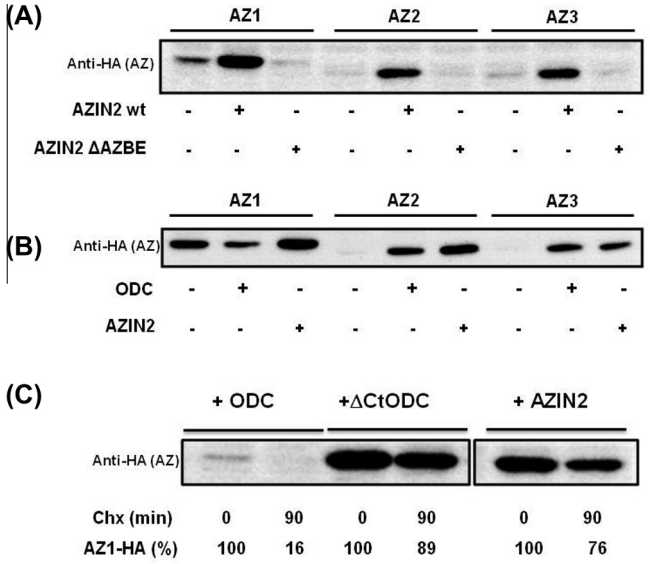

Fig. 8. AZIN2 expression increases the stability of the three antizymes in HEK293 cells. (A) Cells were transiently transfected with each AZ-HA alone, or together with wild type AZIN2 or AZIN2 with deletion of the AZBE region (AZIN2ΔAZBE). Twenty-four h after transfection, cells were lysed and AZ-HA levels were determined by Western blot analysis, using an anti-HA antibody. (B) ODC stabilizes AZ2 and AZ3 but promotes AZ1 degradation. HEK293 cells were transfected with each AZ-HA alone, or together with ODC or AZIN2. AZ expression was analyzed as in A. (C) Differential effect of ODC and C-terminal truncated ODC (ΔCtODC) on AZ1 stability in 293 cells. Cells were transiently transfected with each AZ-HA alone, or together with ODC, ΔCtODC or AZIN2. Twenty hours after transfection, cells were incubated with cycloheximide (100 μM) for 90 min, and after cell lysis AZ1-HA levels were analyzed by Western blotting, using an anti-HA antibody. Results are representative of three separate experiments.

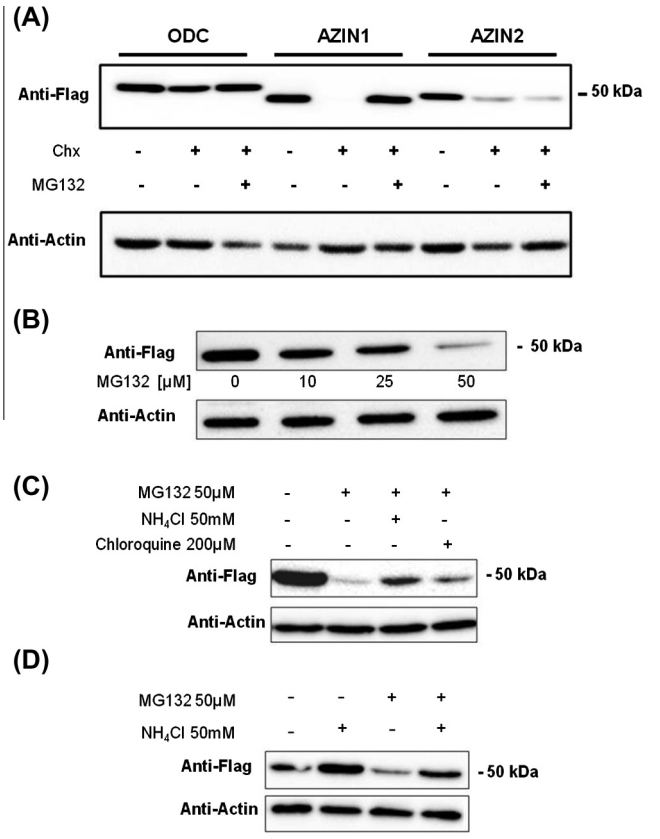

Fig. 9. Effect of the administration of the proteasome inhibitor MG132 on the protein levels of AZIN2 and its paralogues. (A) HEK 293T cells transiently transfected with ODC-FLAG, AZIN1-FLAG or AZIN2-FLAG for 20 h were treated with 100 μM cycloheximide alone or in combination with 50 μM MG132 for additional 4 h. Protein levels were determined by Western blotting and incubation with anti-FLAG antibody. Loading controls were performed using anti-Actin antibody. (B) Twenty hours after transfection of the 293 cells with AZIN2-FLAG, cells were incubated with different doses of MG132 dissolved in DMSO or DMSO alone for additional 4 h, and the expression of AZIN2 was analyzed as described in B. (C) HEK 293T cells transfected with AZIN2-FLAG were incubated for 5 h with no inhibitor or with the proteasomal inhibitor MG132 (50 μM) alone or in combination with inhibitors of lysosomal degradation (ammonium chloride 50 mM, chloroquine 200 μM). (D) HEK 293T cells transfected with AZIN2-FLAG were incubated for 5 h with ammonium chloride (50 mM) or MG132 (50 μM) alone, and with a combination of both compounds. AZIN2 protein levels were assayed as in B. Actin was determined as a loading control. Results shown are representative of at least three separate experiments.

heterodimers with ODC does not allow that AZIN2 might have a negative dominant effect on ODC activity. Whereas ODC may form dimers and AZIN1 may exist as a monomer physiologically [47], our results have shown that AZIN2 is also a monomer. The different ability of ODC and AZIN1 to form dimers has been explained by the existence of substitutions of four essential residues in the putative interface dimer of AZIN1 [63]. However, in the case of AZIN2 these residues are similar to those of ODC, despite the fact that AZIN2 is a monomer. This suggests than in AZIN2 other structural elements must be responsible for its inability to dimerize.

The 3D structure of AZIN2 was predicted by comparative modeling, using known structures of ODC and AZIN1 as templates. As expected, the final model was very similar to those of mouse ODC and AZIN1, mainly in the two main domains (TIM-like α/β-barrel and β-sheet), but differed considerably in the less conserved regions including the N-terminus, C-terminus and some of the loops. In this regard, it should be mentioned that a segment in the N-terminal region of AZIN2 is required for its interaction with the Golgi membranes [51], and that in ODC the C-terminal sequence is critical for the interaction with the proteasome in the antizyme-induced degradation of this enzyme [18].

The comparison of the AZBE regions of the different AZIN2 orthologues recently revealed the existence of seven conserved residues, five of which were equally conserved in the ODC and AZIN1 orthologues (three charged residues K116, K142 and E139; and two non-charged residues A124 and L140) [59]. In the case of mouse AZIN2 the net electric charge of the AZBE region is +2. Given that in previous reports it was postulated that ODC and AZ might interact electrostatically [46,61], the possible influence of the electric charge of the AZBE region of mouse AZIN2 on its interaction with AZ1 can be evaluated from our results with the different variants, in which the conserved residues and hence the electric charge had been modified. According to our data, the substitution of only a single conserved residue of the AZBE region of AZIN2 does not importantly affect the interaction with AZ1, independently of the influence of the substitution on the electric charge of AZBE (decreased in the case of K116A or K142A, maintained in A124S, or increased in E139A). However, double or triple substitutions of conserved residues markedly decreased the interaction of AZIN2 with AZ1, independently of the effects of substitutions on the net electric charge of the AZBE region. These results suggest that charged conserved residues in the AZBE region of AZIN2 are important for the interaction with AZs, independently of the net charge of the region. In this regard, we recently demonstrated that conserved lysines in the AZBE site of ODC are not relevant for the interaction with AZ1 [59]. Remarkably, whereas the substitution of Leu139 impaired critically the function of ODC, affecting the dimerization and the catalytic processes, as well as the interaction with AZs, in the case of AZIN2 the change of this Leu was not critical for the function and the binding to AZs. This discrepancy could be explained by the differences existing in the adjacent residues

surrounding this leucine. Whereas in the case of ODC the Leu139 was surrounded by numerous hydrophobic residues, suggesting the existence of a hydrophobic pocket [62], in the case of AZIN2 this leucine not only was surrounded by hydrophobic amino acids but also by two polar residues, Met and Ser (Fig. 10). These findings suggest that the hydrophobic interactions might be less important in the case of AZIN2, and, therefore, the substitution of this leucine residue is not quite critical for the function of this protein.

The study on the metabolic stability and degradation of AZIN2, and its comparison with those of ODC also showed clear differences between these two homologous proteins. AZIN2 was much more unstable than ODC and, unlike ODC, the presence of any of the three antizymes increased the metabolic stability of AZIN2. Interestingly, AZIN2 also diminished the degradation of all antizyme isoforms, this effect being dependent on the interaction of antizymes with the AZBE region of AZIN2, since the deletion of this segment in AZIN2 abolished the protective effect on AZs. ODC also protected AZ2 and AZ3 against degradation but, however, it promoted the degradation of AZ1. This difference could be related with the major role of AZ1 on ODC degradation by the proteasome in a ubiquitin-independent manner [11,12], in comparison to the roles of AZ2 and AZ3 [19,21]. In addition, whereas it is known that AZ1 is rapidly degraded through a mechanism that requires functional ubiquitin-dependent proteolytic activity [64]), little is known on the degradation of AZ2 and AZ3. Our data indicate that these AZs are also very labile proteins, and that the binding to either AZIN2 or ODC interferes with the degradative pathways of these two AZs. In addition, although it is believed that AZ1 is not degraded together with ODC when presenting the latter to the proteasome [64], our present data suggest that AZ1 can be partially degraded simultaneously to ODC degradation when the ODC-AZ1 complex interacts with the proteasome.

A remarkable difference between the degradative mechanisms of ODC and AZINs is that, whereas the proteasomal degradation of ODC is mediated by AZs in a ubiquitin-independent manner [11,12], AZINs are degraded by the proteasome after ubiquitination [37,48,52], having been demonstrated that AZ1 inhibits ubiquitination of AZIN1 [48]. The protective effect of the three AZs on AZIN2 degradation, shown here, could be exerted by inhibition of AZIN2 ubiquitination. All these facts would explain why when the levels of the three ODC paralogues are higher than those of AZs, ODC is more stable than AZINs. Although, as commented above, AZINs appear to share a common degradative pathway, the differences reported here on the half-lives of AZIN1 and AZIN2 and on the effect of proteasome inhibitor MG132 suggest thatAZIN2 may be also degraded by alternative routes to that of proteasome 26S, such as through the lysosomal degradative pathway, which could gain importance when the proteasomal pathway is inhibited. Similar results have been reported for the degradation of other proteins such as PTEN and IκBα [65,66]. Whether this difference between AZINs may be related to the specific subcellular localization of AZIN2 in ERGIC and vesicle-related structures [39,51] it remains to be confirmed.

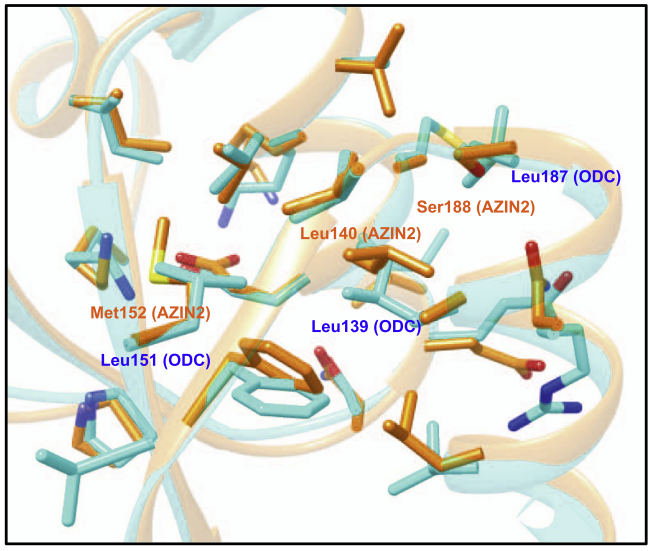

Fig. 10. Visualization of key residues of the AZBE site in the 3D structure of mouse ODC and AZIN2. The figure shows the residues found within a distance of 4 Å from residues L139 and L140 in ODC (blue) and AZIN2 (orange), respectively. This image was produced using UCSF Chimera from the data available in Protein Data Bank for mouse ODC (PDB: 7ODC) and the final model of AZIN2 generated by comparative modeling. Residues were colored according to the type of atom (red, oxygen; blue, nitrogen; yellow, sulfur).

In conclusion, our results indicate that AZIN2 is a monomeric protein, with a 3D structure similar to those of ODC and AZIN1, in which certain conserved residues are important for its interaction with AZs. Like AZIN1, AZIN2 is a short-lived protein that is stabilized upon its interaction with AZs, although under certain conditions other proteolytic systems, besides the 26S proteasome, might be involved in its degradation. Since recent studies have indicated that AZIN2 may have a role in secretory cells [33,36,39], the knowledge of structural aspects of the protein may help to better understand the molecular mechanisms by which AZIN2 may participate in secretion or in other cellular processes where AZIN2 may be implicated.

4. Materials and methods

4.1. Materials

L-[1-^{14}C] ornithine was purchased from Moravek Biochemicals Inc. (Brea, CA). Anti-FLAG M2 monoclonal antibody peroxidase conjugate, anti-HA monoclonal antibody peroxidase conjugate, anti-FLAG affinity gel beads, Igepal CA-630, cycloheximide, suberic acid bis(3-sulfo-N-hydroxysuccinimide ester) sodium salt (BS3), MG132 (Z-Leu-Leu-Leu-al) and chloroquine were obtained from Sigma Aldrich. Lipofectamine 2000 transfection reagent, Dulbecco's Modified Eagle Medium (DMEM), glutamine, fetal bovine serum (FBS) and penicillin/streptomycin were purchased from Invitrogen (Carlsbad, CA). QuickChange site-directed mutagenesis kit was from Stratagene (La Jolla, CA). [1,4-^{14}C] Putrescine (specific activity 107 mCi/mmol) was from Amersham Biosciences. Pierce ECL Plus Western Blotting Substrate was from Thermo Scientific (IL, USA). Primers were purchased from Sigma Genosys.

4.2. Protein structure prediction

Protein sequences were submitted to the GeneSilico metaserver, which is a gateway to a large number of third-party methods that facilitates comparison and interpretation of predictions made by different algorithms [54]. In particular, the metaserver was used for secondary structure prediction and for protein fold-recognition (i.e. alignment of target protein sequence to proteins with experimentally determined structures that can be used as templates for modeling). Fold-recognition alignments reported by primary methods were compared, evaluated, and ranked by the PCONS method [67]. PCONS score >1 in general indicates estimation that the protein fold has been correctly guessed by FR methods. However, lower scores do not necessarily exclude correct predictions, in particular for folds with strongly diverged members. In such cases, a good estimator of prediction quality is the number of occurrences of a given fold at the top positions of the PCONS

ranking [68]. The fold-recognition alignments of murine AZIN2 and the top-scoring templates [PDB: 7odc (murine ODC) and PDB: 3btn (murine AZIN1)] were used as a starting point for modeling of AZIN2 tertiary structure comprising cycles of model building by Modeller [69], evaluation by MetaMQAPII [55], realignment in poorly scored regions as long as manual alignment changes does not improve model quality. Uncertain regions (residues 160–170, 296–312, 342–349 and 418–459) were modeled *de novo* using Refiner [56] in the context of 'frozen' remainder of the AZIN2 model. Coordinates of the model are available for download from the metaserver (ftp://genesilico.pl/iamb/models/AZIN2/).

4.3. Protein model evaluation

For evaluation of models we used two Model Quality Assessment Programs (MQAPs): MetaMQAPII [55] and PROQ [57]. It must be emphasized that MQAP scores only predict the deviation of a model from the real structure (the real deviation can be calculated only by comparison to the real structure, which of course is not available). Thus, the scores reported in this work that indicate e.g. 'extremely good models', must be interpreted as estimations or predictions that our models are 'extremely good', and not as ultimate validation of the model quality. However, it should be mentioned that both PROQ and MetaMQAPII performed very well in various tests and can be regarded as robust predictors.

4.4. Cloning and plasmids

ODC and AZIN2 mouse genes were cloned into the expression vector pcDNA3 (Invitrogen) following standard procedures and the FLAG epitope was introduced to the N terminus of ODC and AZIN2 as described previously [32]. The AZIN2-FLAG construct with a deletion in the antizyme-binding site was generated by PCR and subcloning into pcDNA3 plasmid containing the FLAG epitope [58]. Antizyme constructs with an appropriate deletion of one nucleotide in the frameshifting site, for full-length and functional expression, were obtained by mutagenesis [32]. The HA-tagged constructs ODC-HA and AZ1-HA were generated by introducing the HA epitope to the N terminus of ODC and AZ1, respectively.

4.5. Site-directed mutagenesis

The AZIN2-FLAG construct cloned into the expression vector pcDNA3 was used as template for site-directed mutagenesis using the QuickChange site-directed mutagenesis kit. The AZIN2-FLAG variants generated were K116A, K142A, K116A/K142A, A124S, E139A, L140A, E139A/L140A and E139A/L140A/K142A. In the case of truncated ODC ((ΔCtODC) a stop codon (TGA) was introduced in the position corresponding to C441. All constructs were verified by complete sequencing.

4.6. Cell culture and transient transfections

The monkey kidney fibroblast-like COS7 and the human embryonic kidney (HEK) 293T cell lines were obtained from the ATCC. Both cell lines were cultured in DMEM, containing 10% FBS, 100 units/ml penicillin, and 100 μg/ml streptomycin, in a humidified incubator containing 5% CO_2 at 37 °C. Cells were grown to ~80% confluence. Transient transfections were carried out with Lipofectamine 2000 transfection reagent using 1.5 μl of reagent and 0.3 μg of plasmid per well (12-well plates) in the case of HEK 293T cells and 1 μl of reagent and 0.15 μg of plasmid per well (24-well plates) in the case of COS7 cells. In co-transfection experiments, the mixtures contained equimolecular amounts of each construct. After 6 h of incubation the transfection medium was removed, and fresh complete medium was added, and cells were cultured for 24 h after transfection. The plasmid pcDNA3 without gene insertion was used as negative control.

4.7. Western blot analysis

Transfected cells were collected in PBS, pelleted, lysed in solubilization buffer (50 mM Tris–HCl (pH 8), 1% Igepal and 1 mM EDTA) and centrifuged at 14000×*g* for 20 min. Equal amounts of protein were separated in 10% SDS-PAGE. Gels were transferred to PVDF membranes, blocked with 5% nonfat dry milk in PBS-T (Tween 0.1%), and incubated overnight at 4 °C with the anti-FLAG antibody peroxidase-labeled (1:10000). Immunoreactive bands were detected by using ECL$^+$ detection reagent.

4.8. Cross-linking analysis

HEK 293T cells transfected with ODC-FLAG or AZIN2-FLAG were lysed, and the lysates were incubated for 1 h at 25 °C in 1 mM Tris–HCl, pH 7.5, either alone or with 1 mM bissulfosuccinimidylsuberate (BS3) as crosslinking agent. The cross-linking reaction was terminated by the addition of 1 M Tris–HCl, pH 7.5. Then, the cross-linked material was analyzed by Western blotting and incubation with an anti-FLAG antibody.

4.9. Non-denaturing polyacrylamide gel electrophoresis (PAGE)

Cell lysates from HEK 293T cells transfected with ODC-FLAG and AZIN2-FLAG were mixed in sample buffer (62.5 mM Tris–HCl (pH 6.8), 25% glycerol and 1% bromophenol blue) and separated by PAGE (running buffer and polyacrylamide gels without SDS) at constant current (25 mA/gel) in a cold room until the bromophenol blue reaches the bottom of the gel (about 2 h). Gels were then transferred to PVDF membranes, blocked and incubated with an anti-FLAG antibody.

4.10. Size-exclusion chromatography

HEK 293T cells transfected with ODC-FLAG or AZIN2-FLAG were lysed in solubilization buffer and centrifuged at 14.000×*g* for 20 min, being the supernatant directly injected into a Zorbax Bio Series GF-250 column (Agilent Technologies, CA, USA) in a buffer containing 50 mM Tris, 1 mM EDTA, 4 mM pyridoxal phosphate, and 0.1% Igepal. Sixty 100-μl fractions were collected and analyzed by Western blotting and incubation with anti-FLAG antibody. Bovine serum albumin (Mr 66,000) was used as standard, but in this case fractions were separated by SDS–PAGE and stained with Commasie Blue.

4.11. Immunoprecipitation

HEK 293T cells were transfected with different AZIN2-FLAG variants, alone or in combination with AZ1-HA. 1×10^6 cells were collected in PBS and lysed in 100 μl of solubilization buffer. The samples were centrifuged at 14000×*g* for 20 min, and each supernatant was immunoprecipitated by adding 20 μl of anti-FLAG affinity gel beads. After 3 h incubation, the sample was centrifuged, and the pellet was washed three times with the same solubilization buffer. Elution was performed in 20 μl of 2× electrophoresis sample buffer for 30 min at room temperature. The eluted samples were resolved by SDS–PAGE and analyzed by Western blot.

4.12. ODC activity assay

Transfected HEK 293T cells were collected in PBS, pelleted and lysed in solubilization buffer. The extract was centrifuged at 14000×*g* for 20 min, and ODC activity was determined in the

supernatant. ODC activity was assayed by measuring $^{14}CO_2$ release from L-[1-^{14}C] ornithine [32].

4.13. Polyamine uptake assay

Transient transfected COS7 cells were washed with DMEM (serum-free) and incubated with 200 µl of fresh DMEM (serum-free) containing [1,4-^{14}C] putrescine at a final concentration of 2 µM. After incubation at 37 °C for 20 min, the cells were washed with cold PBS and lysed with trypsin at 37 °C for 30 min. Finally, 3 ml of the scintillation solution was added, and the radioactivity was measured. The nonspecific accumulation of [1,4-^{14}C] putrescine was measured by incubation of the cells with the radioactive compound for 20 min at 4 °C.

Acknowledgements

This work was supported by grants 08681/PI/08 from Seneca Foundation (Autonomous Community of Murcia), SAF2008-03638 from the Spanish Ministry of Science and Innovation, SAF2011-29051 from Spanish Ministry of Economic Affairs and Competitiveness, and FEDER funds from The European Community. BRM and AL were recipients of fellowships from the Ministry of Education, Culture and Sport. BRM was supported by a short-term fellowship from the Federation of European Biochemical Societies (FEBS). AC and JMK were supported by statutory funds of the Adam Mickiewicz University in Poznań, Poland, and JMB was supported by statutory funds of the International Institute of Molecular and Cell Biology in Warsaw and by the European Union (grant POIG.02.03.00-00-003/09). We thank Alejandro Torrecillas (Research Support Service at the University of Murcia) for help with the size-exclusion chromatography experiments.

References

[1] Tabor, C.W. and Tabor, H. (1984) Polyamines. Annu. Rev. Biochem. 53, 749–790.
[2] Thomas, T. and Thomas, T.J. (2001) Polyamines in cell growth and cell death: molecular mechanisms and therapeutic applications. Cell. Mol. Life Sci. 58, 244–258.
[3] Wallace, H.M., Fraser, A.V. and Hughes, A. (2003) A perspective of polyamine metabolism. Biochem. J. 376, 1–14.
[4] Seiler, N. and Raul, F. (2005) Polyamines and apoptosis. J. Cell. Mol. Med. 9, 623–642.
[5] Pegg, A.E. (2009) Mammalian polyamine metabolism and function. IUBMB Life 61, 880–894.
[6] Pegg, A.E. (1988) Polyamine metabolism and its importance in neoplastic growth and a target for chemotherapy. Cancer Res. 48, 759–774.
[7] Auvinen, M., Paasinen, A., Andersson, L.C. and Holtta, E. (1992) Ornithine decarboxylase activity is critical for cell-transformation. Nature 360, 355–358.
[8] Gerner, E.W. and Meyskens, F.L. (2004) Polyamines and cancer: old molecules, new understanding. Nat. Rev. Cancer 4, 781–792.
[9] Pegg, A.E. (2006) Regulation of ornithine decarboxylase. J. Biol. Chem. 281, 14529–14532.
[10] Coffino, P. (2001) Regulation of cellular polyamines by antizyme. Nat. Rev. Mol. Cell. Biol. 2, 188–194.
[11] Murakami, Y., Matsufuji, S., Kameji, T., Hayashi, S., Igarashi, K., Tamura, T., Tanaka, K. and Ichihara, A. (1992) Ornithine decarboxylase is degraded by the 26S proteasome without ubiquitination. Nature 360, 597–599.
[12] Murakami, Y., Matsufuji, S., Hayashi, S., Tanahashi, N. and Tanaka, T. (2000) Degradation of ornithine decarboxylase by the 26S proteasome. Biochem. Biophys. Res. Commun. 267, 1–6.
[13] Mitchell, J.L., Judd, G.G., Bareyal-Leyser, A. and Ling, S.Y. (1994) Feedback repression of polyamine transport is mediated by antizyme in mammalian tissue-culture cells. Biochem. J. 299, 19–22.
[14] Suzuki, T., He, Y., Kashiwagi, K., Murakami, Y., Hayashi, S. and Igarashi, K. (1994) Antizyme protects against abnormal accumulation and toxicity of polyamines in ornithine decarboxylase-overproducing cells. Proc. Natl. Acad. Sci. U.S.A. 91, 8930–8934.
[15] Poulin, R., Casero, R.A. and Soulet, D. (2012) Recent advances in the molecular biology of metazoan polyamine transport. Amino Acids 42, 711–723.
[16] Ivanov, I.P., Gesteland, R.F. and Atkins, J.F. (1998) A second mammalian antizyme: conservation of programmed ribosomal frameshifting. Genomics 52, 119–129.
[17] Mangold, U. (2005) The antizyme family: polyamines and beyond. IUBMB Life 57, 671–676.
[18] Li, X. and Coffino, P. (1993) Degradation of ornithine decarboxylase: exposure of the C-terminal target by a polyamine-inducible inhibitory protein. Mol. Cell. Biol. 13, 2377–2383.
[19] Zhu, C., Lang, D.W. and Coffino, P. (1999) Antizyme2 is a negative regulator of ornithine decarboxylase and polyamine transport. J. Biol. Chem. 274, 26425–26430.
[20] Chen, H., MacDonald, A. and Coffino, P. (2002) Structural elements of antizymes 1 and 2 are required for proteasomal degradation of ornithine decarboxylase. J. Biol. Chem. 277, 45957–45961.
[21] Snapir, Z., Keren-Paz, A., Bercovich, Z. and Kahana, C. (2009) Antizyme 3 inhibits polyamine uptake and ornithine decarboxylase (ODC) activity, but does not stimulate ODC degradation. Biochem. J. 419, 99–103.
[22] Ivanov, I.P., Rohrwasser, A., Terreros, D.A., Gesteland, R.F. and Atkins, J.F. (2000) Discovery of a spermatogenesis stage-specific ornithine decarboxylase antizyme: antizyme 3. Proc. Natl. Acad. Sci. U.S.A. 97, 4808–4813.
[23] Tosaka, Y., Tanaka, H., Yano, Y., Masai, K., Nozaki, M., Yomogida, K., Otani, S., Nojima, H. and Nishimune, Y. (2000) Identification and characterization of testis specific ornithine decarboxylase antizyme (OAZ-t) gene: expression in haploid germ cells and polyamine-induced frameshifting. Genes Cells 5, 265–276.
[24] Kahana, C. (2009) Antizyme and antizyme inhibitor, a regulatory tango. Cell. Mol. Life Sci. 66, 2479–2488.
[25] López-Contreras, A.J., Ramos-Molina, B., Cremades, A. and Peñafiel, R. (2010) Antizyme inhibitor 2: molecular, cellular and physiological aspects. Amino Acids 38, 603–611.
[26] Murakami, Y., Ichiba, T., Matsufuji, S. and Hayashi, S. (1996) Cloning of antizyme inhibitor, a highly homologous protein to ornithine decarboxylase. J. Biol. Chem. 271, 3340–3342.
[27] Nilsson, J., Grahn, B. and Heby, O. (2000) Antizyme inhibitor is rapidly induced in growth-stimulated mouse fibroblasts and releases ornithine decarboxylase from antizyme suppression. Biochem. J. 346, 699–704.
[28] Mitchell, J.L., Simkus, C.L., Thane, T.K., Tokarz, P., Bonar, M.M., Frydman, B., Valasinas, A.L., Reddy, V.K. and Marton, L.J. (2004) Antizyme induction mediates feedback limitation of the incorporation of specific polyamine analogues in tissue culture. Biochem. J. 384, 271–279.
[29] Keren-Paz, A., Bercovich, Z., Porat, Z., Erez, O., Brener, O. and Kahana, C. (2006) Overexpression of antizyme-inhibitor in NIH3T3 fibroblasts provides growth advantage through neutralization of antizyme functions. Oncogene 25, 5163–5172.
[30] Tang, H., Ariki, K., Ohkido, M., Murakami, Y., Matsufuji, S., Li, Z. and Yamamura, K. (2009) Role of ornithine decarboxylase antizyme inhibitor in vivo. Genes Cells 14, 79–87.
[31] Pitkanen, L.T., Heiskala, M. and Andersson, L.C. (2001) Expression of a novel human ornithine decarboxylase-like protein in the central nervous system and testes. Biochem. Biophys. Res. Commun. 287, 1051–1057.
[32] López-Contreras, A.J., López-García, C., Jiménez-Cervantes, C., Cremades, A. and Peñafiel, R. (2006) Mouse ornithine decarboxylase-like gene encodes an antizyme inhibitor devoid of ornithine and arginine decarboxylating activity. J. Biol. Chem. 281, 30896–30906.
[33] Kanerva, K., Lappalainen, J., Mäkitie, L.T., Virolainen, S., Kovanen, P.T. and Andersson, L.C. (2009) Expression of antizyme inhibitor 2 in mast cells and role of polyamines as selective regulators of serotonin secretion. PLoS One 4, e6858.
[34] Mäkitie, L.T., Kanerva, K., Sankila, A. and Andersson, L.C. (2009) High expression of antizyme inhibitor 2, an activator of ornithine decarboxylase in steroidogenic cells of human gonads. Histochem. Cell Biol. 132, 633–638.
[35] Ramos-Molina, B., López-Contreras, A.J., Cremades, A. and Peñafiel, R. (2011) Differential expression of ornithine decarboxylase antizyme inhibitors and antizymes in rodent tissues and human cell lines. Amino Acids 42, 539–547.
[36] López-García, C., Ramos-Molina, B., Lambertos, A., López-Contreras, A.J., Cremades, A. and Peñafiel, R. (2013) Antizyme inhibitor 2 hypomorphic mice. New patterns of expression in pancreas and adrenal glands suggest a role in secretory processes. PLoS One 8, e69188.
[37] Snapir, Z., Keren-Paz, A., Bercovich, Z. and Kahana, C. (2008) ODCp, a brain- and testis-specific ornithine decarboxylase paralogue, functions as an antizyme inhibitor, although less efficiently than AzI1. Biochem. J. 410, 613–619.
[38] Lopez-Contreras, A.J., Ramos-Molina, B., Martínez de la Torre, M., Peñafiel-Verdú, C., Puelles, L., Cremades, A. and Peñafiel, R. (2009) Expression of antizyme inhibitor 2 in male haploid germinal cells suggests a role in spermiogenesis. Int. J. Biochem. Cell. Biol. 41, 1070–1078.
[39] Kanerva, K., Mäkitie, L.T., Bäck, N. and Andersson, L.C. (2010) Ornithine decarboxylase antizyme inhibitor 2 regulates intracellular vesicle trafficking. Exp. Cell Res. 316, 1896–1906.
[40] Mäkitie, L.T., Kanerva, K., Polvikoski, T., Paetau, A. and Andersson, L.C. (2010) Brain neurons express ornithine decarboxylase-activating antizyme inhibitor 2 with accumulation in Alzheimer's disease. Brain Pathol. 20, 571–580.
[41] Solano, F., Peñafiel, R., Solano, M.E. and Lozano, J.A. (1985) Equilibrium between active and inactive forms of rat liver ornithine decarboxylase mediated by L-ornithine and salts. FEBS Lett. 190, 324–328.
[42] Tobias, K.E., Mamroud-Kidron, E. and Kahana, C. (1993) Gly387 of murine ornithine decarboxylase is essential for the formation of stable homodimers. Eur. J. Biochem. 218, 245–250.

[43] Mitchell, J.L. and Chen, H.J. (1990) Conformational changes in ornithine decarboxylase enable recognition by antizyme. Biochim. Biophys. Acta 1037, 115–121.
[44] Li, X. and Coffino, P. (1992) Regulated degradation of ornithine decarboxylase requires interaction with the polyamine-inducible protein antizyme. Mol. Cell. Biol. 12, 3556–3562.
[45] Kern, A.D., Oliveira, M.A., Coffino, P. and Hackert, M.L. (1999) Structure of mammalian ornithine decarboxylase at 1.6 Å resolution: stereochemical implications of PLP-dependent amino acid decarboxylases. Structure 7, 567–581.
[46] Almrud, J.J., Oliveira, M.A., Kern, A.D., Grishin, N.V., Phillips, M.A. and Hackert, M.L. (2000) Crystal structure of human ornithine decarboxylase at 2.1 Å resolution: structural insights to antizyme binding. J. Mol. Biol. 295, 7–16.
[47] Albeck, S., Dym, O., Unger, T., Snapir, Z., Bercovich, Z. and Kahana, C. (2008) Crystallographic and biochemical studies revealing the structural basis for antizyme inhibitor function. Protein Sci. 17, 793–802.
[48] Bercovich, Z. and Kahana, C. (2004) Degradation of antizyme inhibitor, an ornithine decarboxylase homologous protein, is ubiquitin-dependent and is inhibited by antizyme. J. Biol. Chem. 279, 54097–54102.
[49] Cohavi, O., Tobi, D. and Schreiber, G. (2009) Docking of antizyme to ornithine decarboxylase and antizyme inhibitor using experimental mutant and double-mutant cycle data. J. Mol. Biol. 390, 503–515.
[50] Liu, Y.C., Liu, Y.L., Su, J.Y., Liu, G.Y. and Hung, H.C. (2011) Critical factors governing the difference in antizyme-binding affinities between human ornithine decarboxylase and antizyme inhibitor. PLoS One 6, e19253.
[51] Lopez-Contreras, A.J., Sanchez-Laorden, B.L., Ramos-Molina, B., de la Morena, E., Cremades, A. and Peñafiel, R. (2009) Subcellular localization of antizyme inhibitor 2 in mammalian cells: influence of intrinsic sequences and interaction with antizymes. J. Cell. Biochem. 107, 732–740.
[52] Kanerva, K., Mäkitie, L.T., Pelander, A., Heiskala, M. and Andersson, L.C. (2008) Human ornithine decarboxylase paralogue (ODCp) is an antizyme inhibitor but not an arginine decarboxylase. Biochem. J. 409, 187–192.
[53] Grishin, N.V., Osterman, A.L., Brooks, H.B., Phillips, M.A. and Goldsmith, E.J. (1999) X-ray structure of ornithine decarboxylase from *Trypanosoma brucei*: the native structure and the structure in complex with alpha-difluoromethylornithine. Biochemistry 38, 15174–15184.
[54] Kurowski, M.A. and Bujnicki, J.M. (2003) GeneSilico protein structure prediction meta-server. Nucleic Acids Res. 31, 3305–3307.
[55] Pawlowski, M., Gajda, M.J., Matlak, R. and Bujnicki, J.M. (2008) MetaMQAP: a meta-server for the quality assessment of protein models. BMC Bioinformatics 9, 403.
[56] Boniecki, M., Rotkiewicz, P., Skolnick, J. and Kolinski, A. (2003) Protein fragment reconstruction using various modeling techniques. J. Comput. Aided Mol. Des. 17, 725–738.
[57] Wallner, B., Fang, H. and Elofsson, A. (2003) Automatic consensus-based fold recognition using Pcons, ProQ, and Pmodeller. Proteins 53, 534–541.
[58] Lopez-Contreras, A.J., Ramos-Molina, B., Cremades, A. and Peñafiel, R. (2008) Antizyme inhibitor 2 (AZIN2/ODCp) stimulates polyamine uptake in mammalian cells. J. Biol. Chem. 283, 20761–20769.
[59] Ramos-Molina, B., Lambertos, A., López-Contreras, A.J. and Peñafiel, R. (2013) Mutational analysis of the antizyme-binding element reveals critical residues for the function of ornithine decarboxylase. Biochim. Biophys. Acta 1830, 5157–5165.
[60] Hoffman, D.W., Carroll, D., Martinez, N. and Hackert, M.L. (2005) Solution structure of a conserved domain of antizyme: a protein regulator of polyamines. Biochemistry 44, 11777–11785.
[61] Liu, Y.C., Hsu, D.H., Huang, C.L., Liu, Y.L., Liu, G.Y. and Hung, H.C. (2011) Determinants of the differential antizyme-binding affinity of ornithine decarboxylase. PLoS One 6, e26835.
[62] Hoyt, M.A. and Coffino, P. (2004) Ubiquitin-free routes into the proteasome. Cell. Mol. Life Sci. 61, 1596–1600.
[63] Su, K.L., Liao, Y.F., Hung, H.C. and Liu, G.Y. (2009) Critical factors determining dimerization of human antizyme inhibitor. J. Biol. Chem. 284, 26768–26777.
[64] Gandre, S., Bercovich, Z. and Kahana, C. (2002) Ornithine decarboxylase-antizyme is rapidly degrades through a mechanism that requires functional ubiquitin-dependent proteolytic activity. Eur. J. Biochem. 269, 1316–1322.
[65] Tang, Y. and Eng, C. (2006) P53 down-regulates phosphatase and tensin homologue deleted on chromosome 10 protein stability partially through caspase-mediated degradation in cells with proteasome dysfunction. Cancer Res. 66, 6139–6148.
[66] Lee, K.H., Jeong, J. and Yoo, C.G. (2013) Long-term incubation with proteasome inhibitors (PIs) induces IκBα degradation via the lysosomal pathway in an IκB kinase (IKK)-dependent and IKK-independent manner. J. Biol. Chem. 288, 32777–32786.
[67] Lundstrom, J., Rychlewski, L., Bujnicki, J. and Elofsson, A. (2001) Pcons: a neural-network-based consensus predictor that improves fold recognition. Protein Sci. 10, 2354–2362.
[68] Wallner, B. and Elofsson, A. (2007) Prediction of global and local model quality in CASP7 using Pcons and ProQ. Proteins 69, 184–193.
[69] Sali, A. and Blundell, T.L. (1993) Comparative protein modelling by satisfaction of spatial restraints. J. Mol. Biol. 234, 779–815.